

MHD Mixed Convection in Double Lid- Driven Differentially Heated Trapezoidal Cavity

Ahmed F. Khudheyer

Iraq, Baghdad, alnahrainUniversity

ABSTRACT

Mixed convection in a double lid driven trapezoidal cavity with the presence of magnetic field has investigated numerically. The top and bottom walls are both adiabatic, the top wall moves with constant velocity to the left while the bottom wall moves with the same velocity of the top wall to the right. The left wall is maintained at constant hot temperature and the right wall is maintained at constant cold temperature. A finite volume method is used to solve the flow and energy equations. A collocated grid is utilized in the discretization of the governing equations; SIMPLE algorithm is used for coupling the velocity and pressure field. The range of Richardson number is ($0.1 \leq Ri \leq 10$), Hartmann number is ($0 \leq Ha \leq 50$), inclination angles of the side walls of the cavity are ($0, 30^\circ$ and 45°) and Prandtl number is 0.7. The results show that at mixed convection regime ($Ri=1$) and in the absences of magnetic field ($Ha = 0$), the maximum heat transfer occurs for trapezoidal cavity at inclined wall angle (30°).

Keywords: Natural Convection, Trapezoidal Enclosure, Finite Volume

1. INTRODUCTION

MHD natural convection studies are available in literature for both square/rectangular and non-square enclosures. Rudraiah et al. [1] studied the natural convection in a rectangular cavity with the presence of a magnetic field. They concluded that magnetic field decreased the rate of heat transfer. MHD Natural convection in square cavity with partially active vertical walls was studied by Kandaswamy et al. [2]. They concluded that the maximum heat transfer rate occurred at middle-middle thermally active locations and the average Nusselt number decreased with an increase of Hartmann number and increased with an increase of Grashof number. Also MHD natural convection in square or rectangular cavities has been investigated by Garandet et al. [3], Alchaar et al. [4], Kanafer and Chamka [5], and Ece and Büyük [6]. Goutam Saha [7] studied MHD natural convection in a sinusoidal corrugated cavity with discrete isoflux heating from below. He observed that the heat transfer is affected by the heat source sizes for different values of Grashof number and Hartmann number. M. Hasanuzzaman et al. [8] studied MHD natural convection in trapezoidal cavity heated from below. They found that the heat transfer decreased by 20.70% and 16.15% as the inclination angle of side wall increases from 0 to 60 at $Ra=10^5$ and 10^6 respectively. On the other hand, heat transfer decreased by 20.28% and 13.42% as Hartmann number increases from 0 to 50 for $Ra=10^5$ and 10^6 respectively. Amir Houshang Mahmoudi et al. [9] investigated MHD natural convection and entropy generation in a trapezoidal cavity using Cu-water nanofluid. They showed that the enhancement of the Nusselt number due to presence of nanoparticles increases with the Hartman number at $Ra = 10^5$ and 10^6 , but at higher Rayleigh number, a reduction has been observed. In addition it was observed that the entropy generation is decreased when the nanoparticles are present, while the magnetic field generally increases the magnitude of the entropy generation. M. Sheikholeslami et al. [10] investigated MHD natural convection in wavy cavity filled with cu-water nanofluid. The cavity has a sinusoidal wall under constant heat flux. They observed that the Nusselt number increased with an increase of nanoparticles volume fraction, dimensionless amplitude of the sinusoidal wall and Rayleigh number, and decreased with an increase of Hartmann number. Most MHD mixed convection studies are concerned with square cavities in both single and double-sided lid driven. Chamkha [11] studied MHD mixed convection in an isothermally lid driven square cavity in the presence of internal heat generation or absorption. The lid is moved in vertical direction. He found that the flow and the heat transfer inside the cavity are affected by the magnetic field strongly.

2. PROBLEM DESCRIPTION AND MATHEMATICAL MODELING

The geometry of the lid-driven cavity with trapezoidal cross sectional area is described schematically in Fig.1, where the upper and lower boundaries are both adiabatic, the top and the bottom walls move with the same constant velocity to the left of the top wall to the right. The left wall is maintained at constant hot temperature and the right wall is maintained at constant cold temperature.

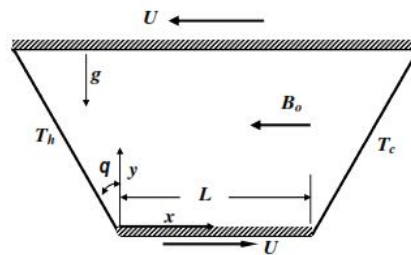


Figure 1 Schematic Diagram of the Physical System.

The trapezoidal-enclosure is constructed with sides of length L . The fluid inside the cavity is capable of conducting current. The top wall of the enclosure is moving with a constant velocity U along the positive x -direction. An external magnetic field of strength B_0 is applied along the x -axis towards the negative side. Air ($Pr = 0.71$) is considered as the working fluid. Although in a strict sense, air is not an electrically conducting fluid, its use is permissible for simulation purposes. The governing induction-less differential equations consisting of mass, momentum and energy in the dimensionless form considering constant fluid properties along with Boussinesq approximation can be expressed as:
For fluid:

$$\frac{\partial U}{\partial X} + \frac{\partial V}{\partial Y} = 0 \quad (1)$$

$$U \frac{\partial U}{\partial X} + V \frac{\partial U}{\partial Y} = -\frac{\partial P}{\partial X} + \frac{1}{Re} \left(\frac{\partial^2 U}{\partial X^2} + \frac{\partial^2 U}{\partial Y^2} \right) \quad (2a)$$

$$U \frac{\partial V}{\partial X} + V \frac{\partial V}{\partial Y} = -\frac{\partial P}{\partial Y} + \frac{1}{Re} \left(\frac{\partial^2 V}{\partial X^2} + \frac{\partial^2 V}{\partial Y^2} \right) - \frac{Ha^2}{Re} + Ri\theta \quad (2b)$$

$$U \frac{\partial \theta}{\partial X} + V \frac{\partial \theta}{\partial Y} = \frac{1}{Re Pr} \left(\frac{\partial^2 \theta}{\partial X^2} + \frac{\partial^2 \theta}{\partial Y^2} \right) \quad (3b)$$

where U, V are the dimensionless velocity components along X and Y directions respectively, P is the pressure, θ is the dimensionless temperatures of fluid, ($Re = V_0 L / \nu$) is the thermodynamic Reynolds number, $N = Ha^2 / Re$ is the interaction parameter with $Ha = B_0 L \sqrt{\sigma / \rho \nu}$ which is hartmann number, $Ri = Gr / Re^2$ is the Richardson number with $Gr = \beta g (T_h - T_c) L^3 / \nu^2$ being the Grashof number.

The dimensional variables are defined as :

$$X = \frac{x}{L}, \quad Y = \frac{y}{L}, \quad U = \frac{u}{U_0}, \quad V = \frac{v}{U_0}, \quad P = \frac{P}{\rho U_0^2}, \quad \theta = \frac{T - T_c}{T_h - T_c} \quad (5)$$

The fluid properties are represented by the density ρ , kinematic viscosity ν , electrical conductivity σ and the thermal diffusivity $\alpha = k_f / \rho C_p$ with k_f and C_p as the fluid thermal conductivity and specific heat respectively. The work due to pressure and viscous dissipation and Hall effect are neglected in the present computation.

The following boundary conditions are imposed:

On the left wall $U=V=0, \theta=1$

On the right wall $U=V=0, \theta=0$

On the top wall: $U=-1, V=0, \frac{\partial \theta}{\partial Y} = 0$

On the bottom wall: $U=1, V=0, \frac{\partial \theta}{\partial Y} = 0$

3. NUMERICAL SOLUTION

The set of conservation equations mass, momentum and energy can be written in general form in Cartesian coordinates as Where Γ is the effective diffusion coefficient, f is the general dependent variable, S_f is the source term. The grid generation scheme based on elliptic partial differential equations is used in the curvilinear coordinates. In this method, the curvilinear coordinates are generated by solving the following elliptic equations.

$$\frac{\partial(Uf)}{\partial X} + \frac{\partial(Vf)}{\partial Y} = \frac{\partial}{\partial X} \left(\Gamma \frac{\partial f}{\partial X} \right) + \frac{\partial}{\partial Y} \left(\Gamma \frac{\partial f}{\partial Y} \right) + S_f$$

$$a = \left(\frac{\partial X}{\partial h} \right)^2 + \left(\frac{\partial Y}{\partial h} \right)^2, \quad g = \left(\frac{\partial X}{\partial V} \frac{\partial X}{\partial h} \right) + \left(\frac{\partial Y}{\partial V} \frac{\partial Y}{\partial h} \right)$$

$$b = \left(\frac{\partial X}{\partial V} \right)^2 + \left(\frac{\partial Y}{\partial V} \right)^2$$

where

$$\left. \begin{aligned} a \frac{\partial^2 X}{\partial V^2} - 2g \frac{\partial^2 X}{\partial V \partial h} + b \frac{\partial^2 X}{\partial h^2} &= 0 \\ a \frac{\partial^2 Y}{\partial V^2} - 2g \frac{\partial^2 Y}{\partial V \partial h} + b \frac{\partial^2 Y}{\partial h^2} &= 0 \end{aligned} \right\}$$

4.VALIDATION

The model validation is an essential part of a numerical investigation. Hence the present numerical results are compared with the numerical results of Iwatsu 1993[12] and Amiri & Khanafer 2011[13] which were reported for mixed convection heat transfer in a trapezoidal enclosure. The comparison is conducted while employing the following dimensionless parameter for Re =100, 400, 1000. Excellent agreement is achieved as illustrated in the following table.

Re	Iwatsu 1993[12]	Amiri & Khanafer2011[13]	Present
100	1.94	2.02	1.95
400	3.84	4.05	3.96
1000	6.33	6.45	6.45

5.RESULTS AND DISCUSSION

The solid line shows the rotational fluid is counterclockwise and the dash lines explain the fluid is rotational in clockwise. Fig.2 shows the effect of Hartmann number on the streamlines for square cavity ($\theta = 0^\circ$) and trapezoidal cavity ($\theta = 30^\circ$ and 45°) at force convection regime where ($Ri=0.1$). In the case of no magnetic field ($Ha=0$) and for the three angles ($\theta = 0^\circ, 30^\circ$, and 45°), the flow field is characterized by a single counterclockwise vortex occupies almost the whole cavity, this vortex is generated by movement of the bottom and the top walls, distortions are observed in the streamlines in the lower right and upper left corners due to impact of fluid to the side walls. As Hartmann number increases from ($Ha=0$) to ($Ha=25$) and for square cavity ($\theta = 0^\circ$), two counterclockwise vortices are generated near the top and bottom walls and clockwise vortex is created in the center of the cavity by buoyancy due to minimize the velocity (force convection effect) in the center of cavity by the presence of magnetic field. For trapezoidal cavity at ($\theta = 30^\circ$ and 45°), the main vortex at ($Ha=0$) is divided into two vortices near the top and bottom walls as Hartmann rises to ($Ha=25$) and two minor vortices are generated by buoyancy near the inclined side walls. As Hartmann increases to ($Ha=50$) and in compare to the case of ($Ha=25$), the velocity in the middle of the cavity is more reduced, this is obvious from enlarging the central clockwise vortex at ($\theta = 0^\circ$), and from merging the two minor vortices near the inclined walls (at $Ha=25$) into one in the middle of the trapezoidal cavity at ($\theta = 30^\circ$ and 45°). Fig.3 shows the effect of Hartmann number on the isotherms for square cavity ($\theta = 0^\circ$) and trapezoidal cavity ($\theta = 30^\circ$ and 45°) at force convection regime where ($Ri=0.1$). For no magnetic field ($Ha=0$), the isotherms are characterized by the thermal boundary layers on the top portion of the left hot wall and the lower portion of the right cold wall. As the Hartmann number increases to ($Ha=25$ and 50) and for the three angles ($\theta = 0^\circ, 30^\circ$, and 45°), plumelike temperature distribution is formed on the left hot wall and on the right cold wall. Fig.4 shows the effect of Hartmann number on the streamlines for square cavity ($\theta = 0^\circ$) and trapezoidal cavity ($\theta = 30^\circ$ and 45°) at mixed convection regime where ($Ri=1$). For the case of no magnetic field ($Ha=0$) and for square cavity ($\theta = 0^\circ$), the streamlines are characterized by two counterclockwise vortices in the top and bottom of the cavity, and two minor clockwise vortices form near the side walls, the minor vortices are generated by natural convection effect. For trapezoidal cavity at angles ($\theta = 30^\circ$, and 45°) and in compare with square cavity ($\theta = 0^\circ$), the two minor vortices near the side walls are disappeared and the streamlines are characterized by single

counterclockwise vortex, so that the angles ($\theta=30^\circ$, and 45°) minimize the effect of natural convection and sustain the effect of the moving horizontal walls. As Hartmann number increases to ($Ha=25$) for square cavity ($\theta=0^\circ$) and trapezoidal cavity ($\theta=30^\circ$), the moving walls effect in the middle of cavity decreases and a clockwise vortex appears in the middle of cavity and two counterclockwise vortices appear near top and bottom walls. For trapezoidal cavity at ($\theta=45^\circ$), minor clockwise vortex appears near the left inclined wall. Further, as Hartmann number increases to ($Ha=50$), the central clockwise vortices at angles ($\theta=0^\circ$, 30° , and 45°) are enlarged due to the increasing of the applied magnetic field. Effects of Hartmann number on the isotherms at ($Ri=1$) for the three angles ($\theta=0^\circ$, 30° , and 45°) are shown in Fig.5. In the absence of magnetic field ($Ha=0$), for square cavity ($\theta=0^\circ$), the isotherms are characterized by plumelike temperature distribution on both hot and cold side walls. For trapezoidal cavity ($\theta=30^\circ$ and 45°) at ($Ha=0$), the plume is disappeared, and the thermal boundary layers are formed along both side walls. As Hartmann rises to ($Ha=25$ and 50) for the square cavity ($\theta=0^\circ$), similar distribution of isotherms to the case of ($Ha=0$) can be seen, for trapezoidal cavity ($\theta=30^\circ$ and 45°) plumes are formed on both the hot and the cold side walls. Fig.6 shows the effect of Hartmann number on the streamlines for square cavity ($\theta=0^\circ$) and trapezoidal cavity ($\theta=30^\circ$ and 45°) at natural convection regime where ($Ri=10$). In the absence of magnetic field ($Ha=0$), for the three angles ($\theta=0^\circ$, 30° , and 45°), the flow field is characterized by counterclockwise shear vortices near the moving horizontal walls, and clockwise vortex at the center of the cavity which is generated by buoyancy. It is interesting to note that the upper shear vortex near the upper wall at angles (30° , and 45°) expands horizontally due to the diverging of the cavity. Since the magnetic field suppresses the velocity in almost the entire cavity except near the moving horizontal walls, the streamlines are more clustered toward the moving walls as Hartmann number increase to ($Ha=25$ and 50). Effects of Hartmann number on the isotherms at ($Ri=10$) for the three angles ($\theta=0^\circ$, 30° , and 45°) are shown in Fig.7. In the absence of magnetic field ($Ha=0$), for the three angles ($\theta=0^\circ$, 30° , and 45°), the thermal boundary layers are formed on the lower portion of the left hot wall and the top portion of the right cold wall. As Hartmann rises to ($Ha=25$ and 50) for the three angles ($\theta=0^\circ$, 30° , and 45°), the isotherms tend to be parallel to the side walls, this means that the mode of heat transfer is conduction.

6. AVERAGE NUSSOLT NUMBER

Figs. 8, 9, and 10 show the variation of average Nusselt number from the hot left side wall with Hartmann number for Richardson numbers $Ri=0.1$, 1 , and 10 respectively. In the forced convection regime ($Ri=0.1$), in the absence of magnetic field ($Ha=0$), the maximum heat transfer occurs at square cavity ($\theta=0^\circ$), and Nusselt number decreases with Hartmann number increases for square cavity ($\theta=0^\circ$) and trapezoidal cavity ($\theta=30^\circ$ and 45°). In the Mixed convection regime ($Ri=1$), in the absence of magnetic field ($Ha=0$), the maximum heat transfer occurs at trapezoidal enclosure ($\theta=30^\circ$), and Nusselt number decreases with Hartmann increases for square cavity ($\theta=0^\circ$) and trapezoidal cavity ($\theta=30^\circ$ and 45°). In the natural convection regime ($Ri=0$), in the absence of magnetic field ($Ha=0$), the maximum heat transfer occurs at square enclosure ($\theta=0^\circ$), and Nusselt number almost constant for Hartmann number ($Ha \geq 25$) for square ($\theta=0^\circ$) and trapezoidal cavity ($\theta=30^\circ$ and 45°).

7. CONCLUSIONS

1. In the forced convection regime ($Ri=0.1$), in the absence of magnetic field ($Ha=0$), the maximum heat transfer occurs at square cavity ($\theta=0^\circ$), and Nusselt number decreases with Hartmann number increases for square cavity ($\theta=0^\circ$) and trapezoidal cavity ($\theta=30^\circ$ and 45°).
2. In the mixed convection regime ($Ri=1$), in the absence of magnetic field ($Ha=0$) and for square cavity ($\theta=0^\circ$), the isotherms are characterized by plumelike temperature distribution on both hot and cold side walls.
3. In the mixed convection regime ($Ri=1$), in the absence of magnetic field ($Ha=0$) and for trapezoidal cavity ($\theta=30^\circ$ and 45°), the plumelike is disappeared, and the thermal boundary layers are formed along both side walls.
4. At ($Ri=1$), the angles ($\theta=30^\circ$, and 45°) minimize the effect of natural convection and sustain the effect of the moving horizontal walls.
5. In the Mixed convection regime ($Ri=1$), in the absence of magnetic field ($Ha=0$), the maximum heat transfer occurs at trapezoidal enclosure ($\theta=30^\circ$), and Nusselt number decreases with Hartmann increases for square cavity ($\theta=0^\circ$) and for trapezoidal cavity ($\theta=30^\circ$ and 45°).
6. In the natural convection regime ($Ri=0$), in the absence of magnetic field ($Ha=0$), the maximum heat transfer occurs at square enclosure ($\theta=0^\circ$), and Nusselt number is almost constant for Hartmann number ($Ha \geq 25$) for square ($\theta=0^\circ$) and for trapezoidal cavity ($\theta=30^\circ$ and 45°).

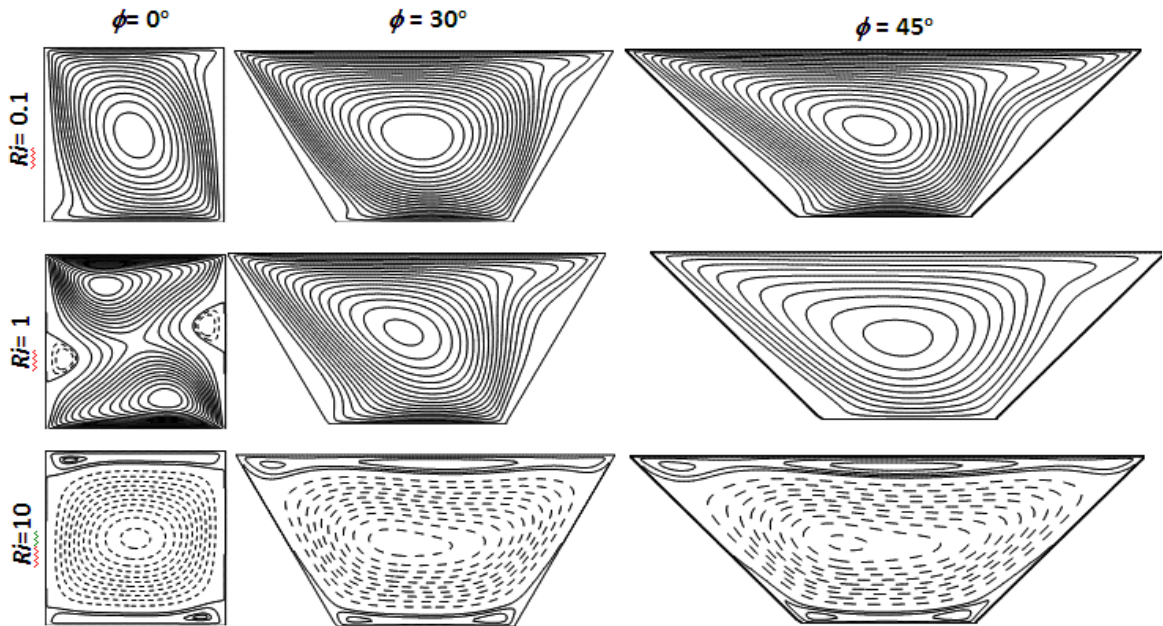


Figure 2 Streamlines for various Richardson numbers and cavity angles at Ha=0

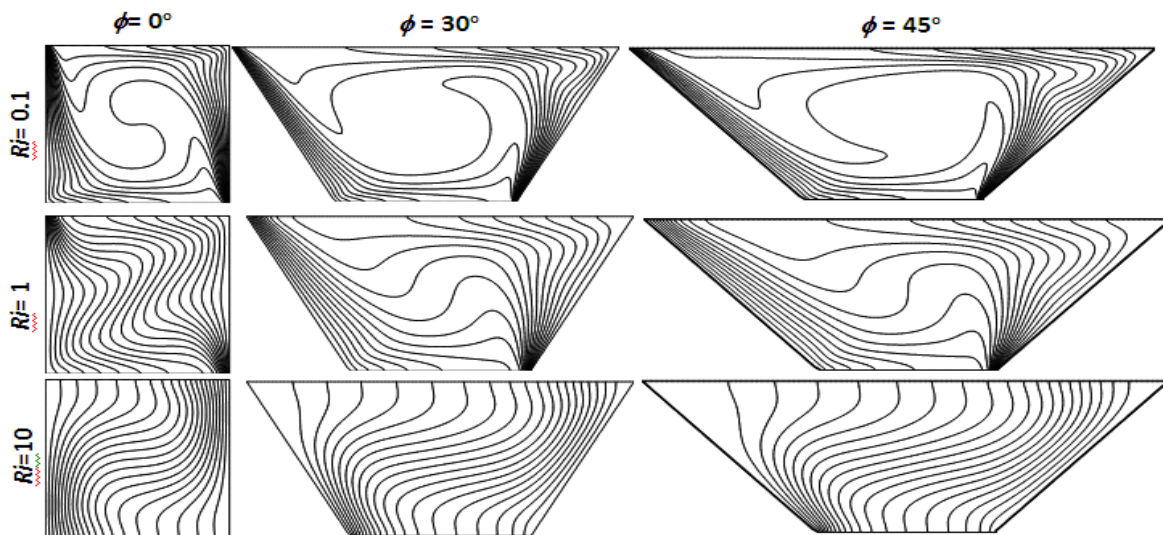


Figure 3 Isotherms for various Richardson numbers and cavity angles at Ha=0

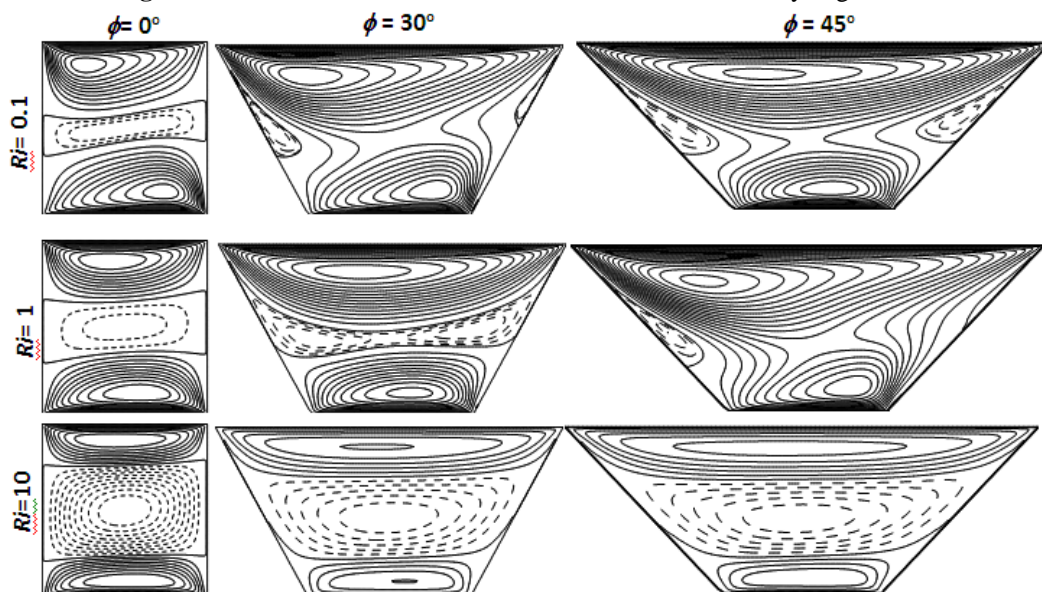


Figure 4 Streamlines for various Richardson numbers and cavity angles at Ha=25

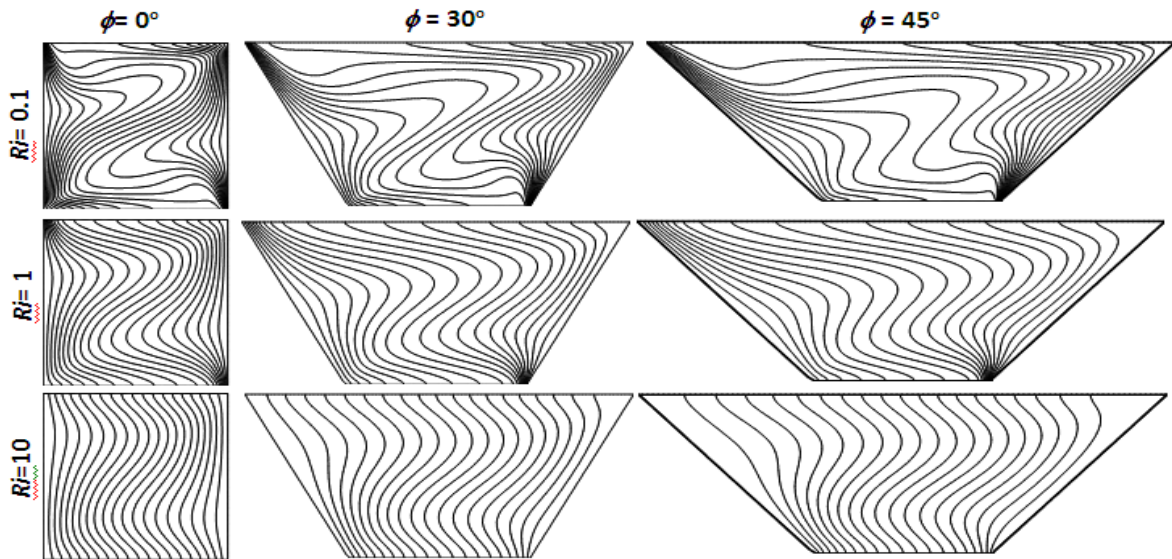


Figure 5 Isotherms for various Richardson numbers and cavity angles at Ha=25

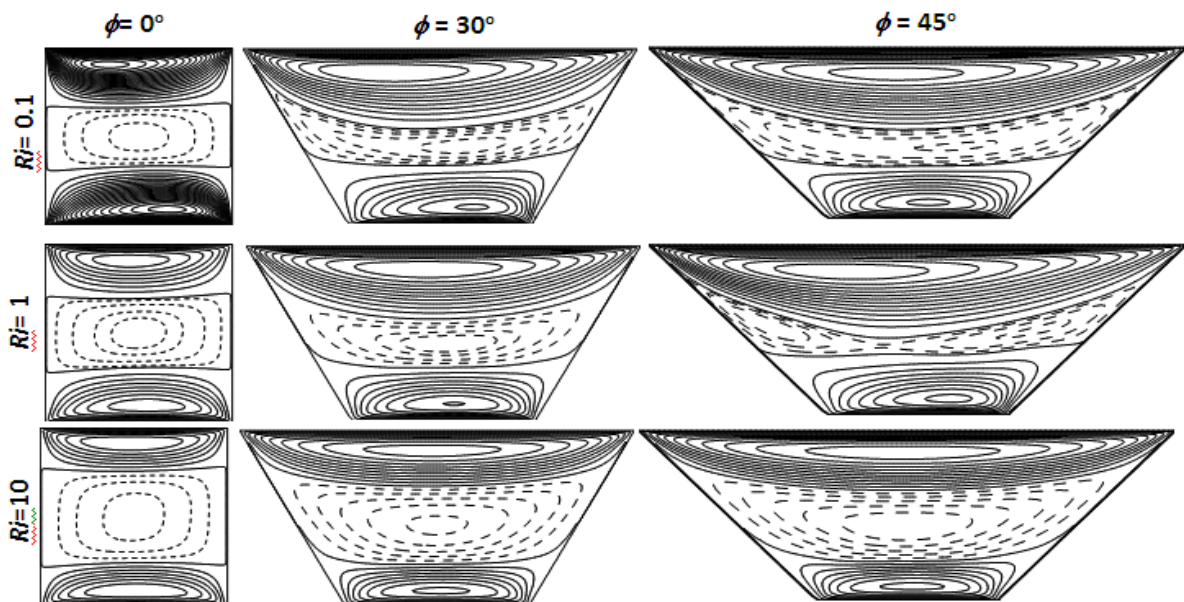


Figure (6) Streamlines for various Richardson numbers and cavity angles at Ha=50

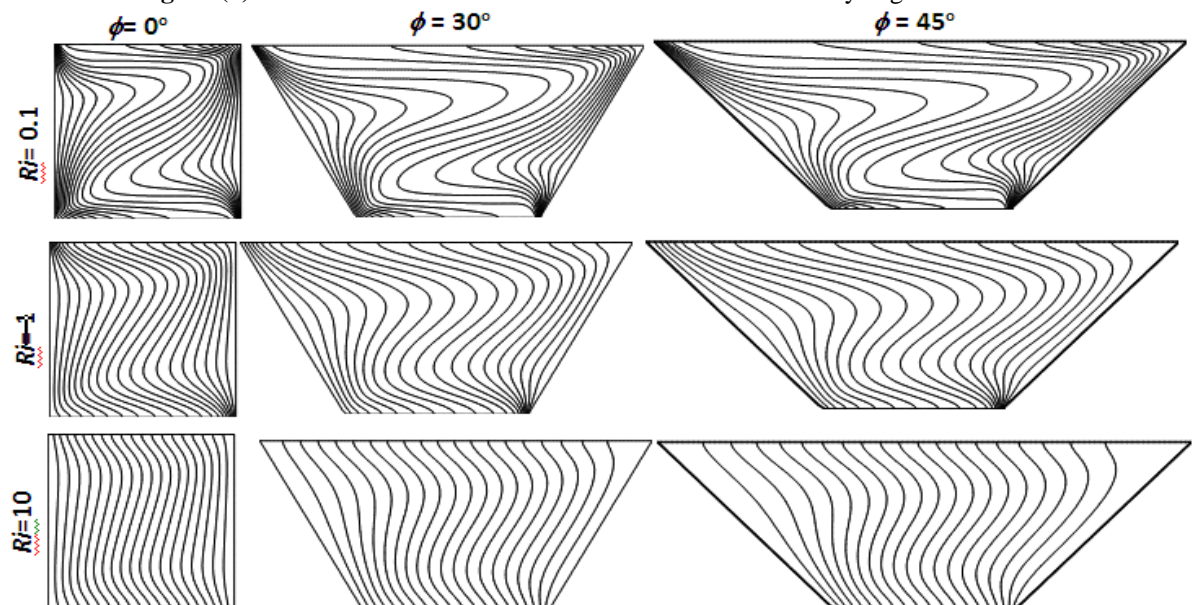


Figure (7) Isotherms for various Richardson numbers and cavity angles at Ha=50

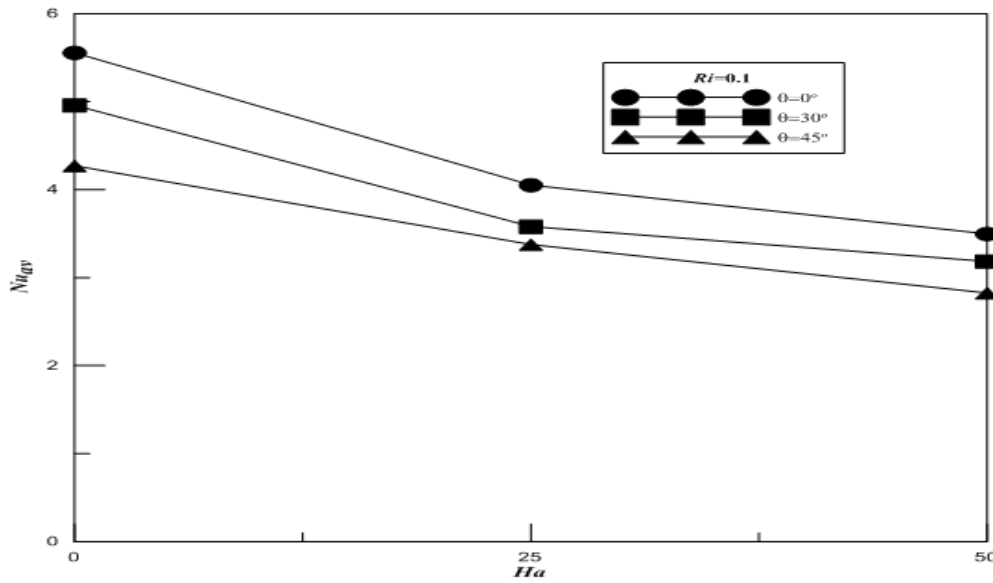


Figure 8 shows the variation of average Nusselt number from the hot left side wall with Hartmann number for Richardson numbers $Ri=0.1$.

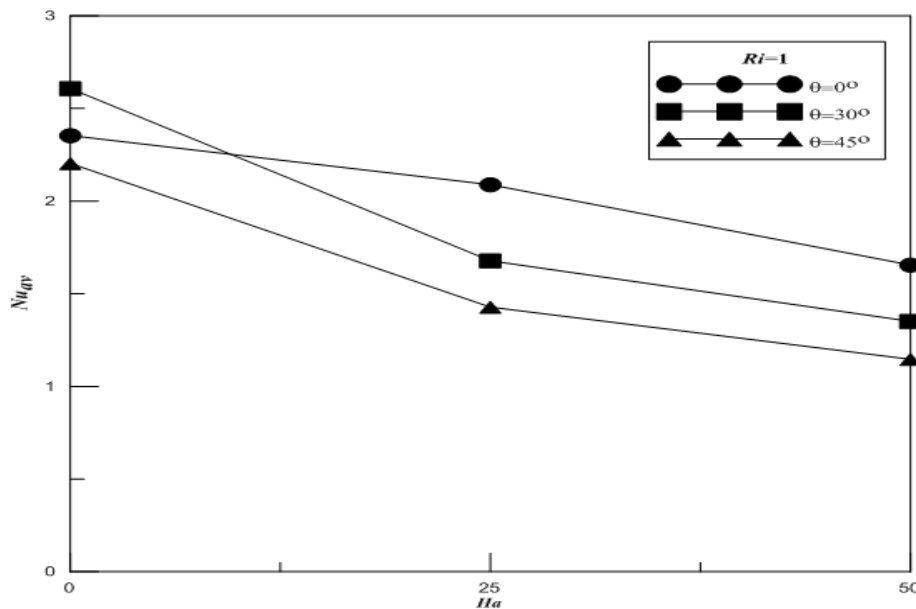


Figure 9 shows the variation of average Nusselt number from the hot left side wall with Hartmann number for Richardson numbers $Ri=1$.

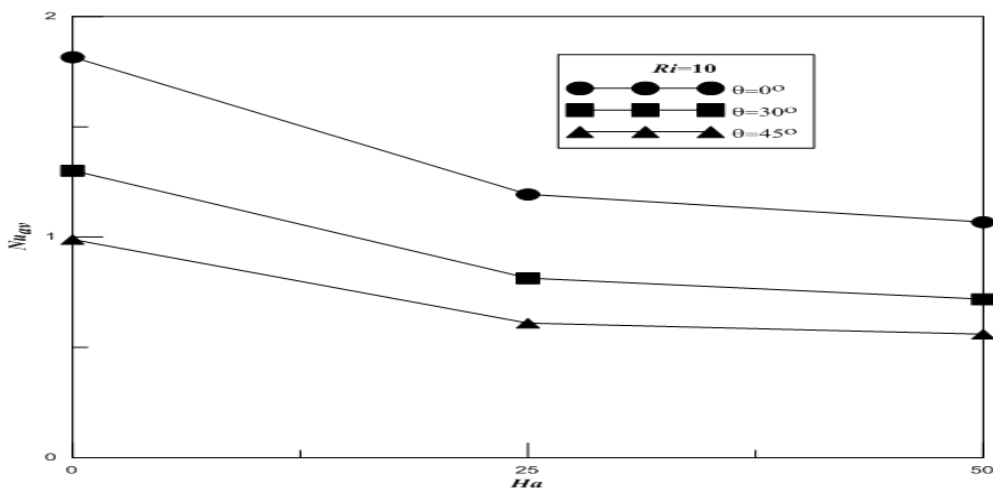


Figure 10 shows the variation of average Nusselt number from the hot left side wall with Hartmann number for Richardson numbers $Ri=10$.

REFERENCE

- [1] N. Rudraiah, R.M. Barron, M.V. Enkatachalappa, C.K. Subbaraya, Effect of a magnetic field on free convection in a rectangular enclosure, *Int. J. Eng. Sci.* 33 (1995)1075–1084.
- [2] Kandaswamy P., Sundari S. M. and Nithyadevi N., (2008) Magnetoconvection in an enclosure with partially active vertical walls, *Int. J. of Heat and Mass Transfer* 51, 1946-1954.
- [3] J.P. Garandet, T. Alboussiere, R. Moreau, Buoyancy driven convection in a rectangular enclosure with a transverse magnetic field, *Int. J. Heat Mass Transfer* 35 (1992)741–748.
- [4] S. Alchaar, P. Vasseur, and E. Bilgen, Natural Convection Heat Transfer in a Rectangular Enclosure with a Transverse Magnetic Field, *ASME Journal of Heat Transfer*, vol. 117, pp. 668±673, 1995.
- [5] Khanafer, K., Chamkha, A.J., 1999. Mixed convection flow in a lid-driven enclosure filled with a fluid-saturated porous medium. *Int. J. Heat Mass Transfer* 42,2465–2481.
- [6] Ece M.C., Büyük E. (2006); "Natural-Convection Flow under a Magnetic Field in an Inclined Rectangular Enclosure Heated and Cooled on Adjacent Wall", *Fluid Dynam. Res.*, 38, 564–590.
- [7] G. Saha, "Finite element simulation of magnetoconvection inside a sinusoidal corrugated enclosure with discrete isoflux heating from below" *Int. Comm. Heat Mass Transfer* 37 (2010) 393-400.
- [8] M. Hasanuzzaman , Hakan F. Öztop , M.M. Rahman , N.A. Rahim , R. Saidur , and Y. Varol "Magneto-hydrodynamic natural convection in trapezoidal cavities" *International Communications in Heat and Mass Transfer* 39 (2012) 1384–1394
- [9] Amir Houshang Mahmoudi, Ioan Pop, Mina Shahi, and Farhad Talebi "MHD natural convection and entropy generation in a trapezoidal enclosure using Cu–water nanofluid" *Computers & Fluids* 72 (2013) 46–62.
- [10] M. Sheikholeslami, M. Gorji-Bandpy, D.D. Ganji, and Soheil Soleimani " Natural convection heat transfer in a cavity with sinusoidal wall filled with CuO–water nanofluid in presence of magnetic field" *Journal of the Taiwan Institute of Chemical Engineers* 45 (2014) 40–49.
- [11] A.J. Chamkha, Hydromagnetic combined convection flow in a vertical lid driven cavity with internal heat generation or absorption, *Numer. Heat Transfer A* 41 (2002) 529–546.
- [12] Reima Iwatsu, Jae Min Hyun, and Kunio Kuwahara " mixed convection in a driven cavity with a stable vertical temperature gradient" *int.j.heat and mass transfer* vol 36. No.6. PP 1601-1608, 1993.
- [13] Amiri & Khanafer, fluid structure interaction analysis of mixed heat transfer in a lid-driven cavity with flexible bottom wall, *J. Heat Transfer* 54,(2011), 3826-3836.

AUTHOR



Ahmed F. Khudheyer, born in Iraq, 1974, and he received the B.S. and M.S. degrees in Mechanical Engineering from University of Technology in 1997 and 2000, respectively, and Ph.D in mechanical engineering from Baghdad University in 2006. He now with Al-Nahrain University